Concentration of Intracellular Hepatic Apolipoprotein E in Golgi Apparatus Saccular Distensions and Endosomes

S. Dahan, J. P. Ahluwalia, L. Wong,‡ B. I. Posner,* and J. J. M. Bergeron

Department of Anatomy and Cell Biology and *Department of Medicine, McGill University, Montreal, Quebec, Canada H3A 2B2; and ‡Department of Physiology, Louisiana State University Medical Center, New Orleans, Louisiana 70112-2865

Abstract. The intrahepatic distribution of apolipoprotein E has been assessed by immunogold labeling of cryosections as well as by Western blotting of organelles isolated from liver homogenates. Both techniques supported the prior analytical fractionation studies of Wong (1989) who concluded that intrahepatic apoE was largely endosomal. All endosomal components decorated by gold particles indicative of apoE antigenicity in cryosections appeared filled with lipoprotein-like particles thereby accounting for this prominent morphological feature of isolated liver endosomes. The distribution of gold particles about the hepatic Golgi apparatus revealed a high content of apoE in closely apposed endosomes, ca. 400 nm in diameter, double labeled for apoE and internalized HRP. Remarkably, apoE (but not internalized HRP) was also observed within saccular distensions of all saccules of stacked Golgi cisternae but absent from the flattened saccular components as was also observed for apoB. This contrasted with albumin, the major secretory protein, which was uniformly distributed throughout the hepatic Golgi apparatus. These observations support a growing body of evidence for intra-Golgi sorting of secretory material in hepatic Golgi apparatus. The lack of any immunoreactive apoE or albumin in small 70–90 nm vesicles about the Golgi cisternae suggests limits to current models of vesicle-mediated intra-Golgi transport.

THE hypothesis of protein secretion was originally elaborated as a consequence of interpreting morphologically observed compartments, i.e., the ER, Golgi apparatus and secretory vesicles which were postulated to act sequentially in the synthesis, transport, and packaging of proteins destined for extracellular discharge by exocytosis (Palade, 1975). Extensive morphological studies have been carried out on the exocrine pancreas and rat liver due to the ease of visualization of their respective secretory contents (Claude, 1970; Ehrenreich et al., 1973; Palade, 1975; Novikoff and Yam, 1978). Using protein A–gold labeling of tissue sections, the secretory pathway of exocrine pancreas was substantiated (Geuze et al., 1979; Bendayan, 1984). In particular this technique was instrumental in ruling out a cytosolic pathway of zymogen secretion which had been previously proposed on pharmacological grounds (cf. Palade, 1975; Rothman, 1975).

In liver parenchyma, the major secretory components visualized are lipoprotein particles. Although originally considered to be a morphological marker for the hepatic Golgi apparatus (Ehrenreich et al., 1973) debate has continued as to the delineation of the compartments in the Golgi region of the hepatocyte which concentrate lipoprotein particles. A confounding aspect was the identification of compartments accumulating insulin or prolactin via receptor-mediated endocytosis as Golgi components due to their location, lipoprotein-like content, and lack of the lysosomal marker acid phosphatase (Bergeron et al., 1979, 1983) or multivesicular bodies with a mottled content for asialoorosomucoid internalization (Wall et al., 1980) which were also interpreted by Haimes et al. (1981) as intraluminal lipoprotein.

The major protein constituents of liver-derived lipoproteins, i.e., very low density lipoprotein (VLDL),[1] are apolipoproteins B and E (apoB and apoE) (Zannis et al., 1993). By analytical subcellular fractionation of liver homogenates, Wong estimated that ca. 60% of intrahepatic apoE was derived from endocytosis with the majority found in endosomes (Wong, 1989). Since lipoprotein-like particles are a prominent morphological feature of endosome preparations isolated from liver parenchyma (Posner et al., 1982; Khan et al., 1982, 1986; Lai et al., 1989), a dual location for lipoproteins in liver parenchyma has been proposed, i.e., in both Golgi secretory components as well as in endosomal

Address all correspondence to J. J. M. Bergeron, Department of Anatomy and Cell Biology, McGill University, Montreal, Quebec, Canada H3A 2B2. Ph.: (514) 398-6351. Fax: (514) 398-5047.

1. *Abbreviations used in this paper*: ApoE, apolipoprotein E; CI-MPR, cation-independent mannose 6-phosphate receptor; Gav, Golgi-associated vesicle; Gi, Golgi intermediate; lgp120, lysosomal membrane glycoprotein 120; LDL, low density lipoprotein; Li, light mitochondrial intermediate; MVE, multivesicular endosome; RT, room temperature; VLDL, very low density lipoprotein.

components some of which aggregate close to the Golgi apparatus (Bergeron et al., 1983, 1985; Kay et al., 1984).

Recently, Hamilton et al. (1990) have carried out an immunocytochemical analysis of apoE distribution in rat liver parenchyma. Remarkably, these authors concluded that apoE was distributed in the cytosol and peroxisomes as well as in elements of the secretory (ER, Golgi apparatus) and endocytic apparatus (multivesicular bodies) as well as the cell surface and a small amount in mitochondria. This led to the proposal that apoE would act as a sterol carrier enabling the interorganellar transport and exchange of cholesterol for membrane biogenesis and/or sterol modification reactions.

Using a well-characterized antiserum to apoE (Wong and Rubenstein, 1977), we were unable to confirm the localization studies of Hamilton et al. (1990). ApoE was beyond detection in cytosol or peroxisomes. As predicted from the studies of Wong (1989) apoE was highly concentrated in the endosomal apparatus (but not lysosomes) including endosomes within 100 nm of Golgi apparatus. Golgi apparatus was also highly enriched in apoE. Here, however apoE was segregated to dilated distensions of all Golgi saccules, which also concentrated apoB, but was not detected in the contiguous flattened saccular compartment of the Golgi stack or in any putative transport vesicles of 60–90 nm in diameter postulated to ferry secretory proteins between adjacent Golgi cisternae. These studies raise questions about the current postulated role for apoE in intracellular cholesterol transport among organelles as well as the nature of the vehicle responsible for the intra-Golgi transport of apoE.

Materials and Methods

Materials

Percoll was obtained from Pharmacia LKB Biotechnology (Montreal, Quebec). Protein assay dye reagent, chemicals and molecular weight markers used in SDS-PAGE were obtained from Bio-Rad Canada Ltd. (Mississauga, Ontario). Somnotol was from M.T.C. Pharmaceuticals (Cambridge, Ontario). Methyl cellulose was from Anachemia Chem. Inc. (Lab Grade, Ac5900; Montreal, Quebec). Nitrocellulose paper (BA85) was from Schleicher & Schuell (Keene, NH). Casein (Hammarsten grade) was from BDH Chemicals Canada Ltd. (Montreal, Quebec). Polyoxyethylene sorbitan monolaureate (Tween-20) was from Sigma Chemical Co. (St. Louis, MO) and ^{125}I-labeled goat anti-rabbit IgG was obtained from New England Nuclear Research Products (Mississauga, Ontario). All other chemicals were obtained from commercial sources and were of reagent grade.

Male and female Sprague Dawley rats (100–150 g) were purchased from Charles River Canada Ltd. (St. Constant, Quebec).

Isolation of Subcellular Fractions

To obtain light mitochondrial (Li) and Golgi intermediate (Gi) fractions, rat livers were homogenized in 0.25 M sucrose containing 4 mM imidazole (used for all sucrose solutions), pH 7.4, essentially as described by Khan et al. (1986). Density of the fractions was determined at 22°C using an Abbe II refractometer (Cambridge Instruments Inc., Buffalo, NY).

Rat liver lysosome fraction L2 (Lys) was isolated by isopycnic centrifugation in a metrizamide step density gradient, according to the method of Wattiaux et al. (1978) with an enrichment of acid phosphatase of 81-fold determined (relative specific activity). Rough ER was prepared by the protocol of Walter and Blobel (1983) as described previously (Wada et al., 1991; Ou et al., 1992). The cytosolic fraction (S) was isolated by differential centrifugation as previously described (Authier et al., 1994). Combined endosomes (EN) were prepared by discontinuous sucrose gradients according to the method of Authier et al. (1994). The peroxisomal fraction (18.6-fold enrichment of catalase over the homogenate) and the mitochondrial fraction (7.5-fold enrichment of cytochrome c oxidase over the homogenate), generous gifts from Dr. R. A. Rachubinski (University of Alberta, Edmonton, Alberta, Canada), were prepared as described by Bodnar and Rachubinski (1991) and characterized as detailed in Authier et al. (1994). Protein in subcellular fractions was determined by the method of Bradford (1976).

Antibodies

Antiserum to lysosomal membrane glycoprotein, lgp120, was a gift of Dr. I. Mellman (Yale University, New Haven, CT). The rabbit polyclonal anti-cation-independent mannose 6-phosphate receptor (CI-MPR) antibody was generously supplied by Dr. P. Nissley (National Institutes of Health, Bethesda, MD). The control polyclonal antibody, rabbit anti-α-amylase, was from Dr. M. Bendayan (University of Montreal, Quebec). Goat anti-rabbit IgG-10 nm gold was from Sigma Chemical Co. (St. Louis, MO) while goat anti-mouse IgG-5 nm gold was from E-Y Labs (Montreal, Quebec). Rabbit polyclonal anti-human catalase antibody was purchased from Calbiochem-Behring Corp. (La Jolla, CA), rabbit polyclonal anti-rat albumin (IgG fraction) was obtained from Cappel Laboratories (West Chester, PA), and mouse polyclonal anti-peroxidase antibody was from Bio-Can Scientific Inc. (Mississauga, Ontario).

Immunoblotting

Subcellular fractions of liver homogenates were subjected to electrophoresis on a discontinuous system using 8% polyacrylamide gels, electrophoretically transferred to nitrocellulose paper (0.45 μm pore size) in a Hoefer Transfor (Hoefer Scientific Instruments, San Francisco, CA) according to the technique of Towbin et al. (1979). Electrophoretic transfer was carried out at 380 mA for 90 min in transfer buffer containing 25 mM Tris base and 192 mM glycine. The non-specific binding sites were quenched by incubation overnight at room temperature (RT) in 300 mM NaCl, 10 mM Tris-HCl, pH 7.4, containing 5% skim milk and 0.05% Tween 20 (buffer TWA). The blots were subsequently incubated for 3 h at RT with antiserum to apoE diluted 1:1,200 to 1:200 in buffer TWA (buffer A), washed three times over a period of 1 h at RT with buffer TWA containing 0.5% skim milk. The bound immunoglobulin was detected using ^{125}I-labeled goat anti-rabbit IgG and washed in buffer TWA as above. Molecular weights of immunoreactive bands were estimated by running protein standards (Bethesda Research Laboratories, Bethesda, MD).

Electron Microscopy

Fixation, Cryoprotection, and Freezing. Male Sprague-Dawley rats (100–125 g), fasted overnight, were used. Animals were anesthetized with somnotol. Livers were perfused with Ringer's lactate solution at 10 ml/min using a minipuls 2 pump (Gilson Minipuls® Peristaltic Pumps, Mandel Scientific Company Ltd., Lachine, Quebec, Canada) after cannulation of the portal vein and incision of the inferior vena cava. Perfusion with Ringer's solution was carried out until the liver visibly blanched (usually <30 s) and was followed by perfusion-fixation with freshly prepared 4% paraformaldehyde/0.5% glutaraldehyde in 0.1 M phosphate buffer (pH 7.4). After 10 min of perfusion-fixation, small pieces of liver (1 mm^3) were removed and immersed in the same fixative for 1 h at 4°C. The small pieces of liver were washed with 4% sucrose/0.1 M phosphate buffer and equilibrated for 30 min to 1 h with 2.3 M sucrose (Tokuyasu, 1980). Tissues were frozen directly in liquid nitrogen.

For double-labeling studies, overnight-fasted female Sprague-Dawley rats (180–200 gm) were anesthetized with somnotol. After an abdominal incision, anesthetized rats were injected intraportally with 1 mg HRP/100 g body weight (type VI; Sigma Chem. Co.) dissolved in PBS containing 2.5% BSA (1 mg HRP/100 ml). 10 or 30 min after the intraportal injection, livers were perfusion-fixed and the tissue prepared as described above.

Tissue Sectioning and Immunolabeling. All subsequent steps were based on the procedures of Tokuyasu (1978, 1980), Griffiths et al. (1982, 1983, 1984) and Geuze et al. (1984). Tissue stubs were sectioned in a Reichert-Jung ultramicrotome equipped with an FC4D cryochamber. Formvar-coated copper grids (200 mesh) were carbon coated and then rendered hydrophilic using a glow-discharge apparatus. Sections were cut at −100°C, picked up with a copper loop filled with a 2.3 M sucrose solution, and transferred to grids. The grids were then kept on drops of PBS (137 mM NaCl, 2.7 mM KCl, 1.5 mM KH_2PO_4, 6.5 mM Na_2HPO_4, pH 7.4) containing 2% bovine serum albumin, 2% casein, and 0.5% ovalbumin (PBS-BCO block) on ice until use (usually <5 h). All the subsequent steps were performed at RT and on the same day. Non-specific binding sites were blocked by PBS-BCO block and free aldehyde groups of the fixative were blocked by floating the grids on drops of PBS containing 0.02 M glycine for 15 min.

For single-labeling experiments, sections were incubated for 30 min at RT with primary antibody (or overnight at 4°C for the anti-CI-MPR antibody) at appropriate dilutions (see below) and washed six times with PBS for a total of 30 min. Non-specific sites were blocked with PBS-BCO, and the sections were then incubated with secondary antibodies conjugated to colloidal gold (see figure legends) and washed as above.

Side-by-side control experiments for apoE labeling specificity were carried out using an anti-amylase antibody at 1:200 dilution. In compartments strongly labeled for apoE, the mean gold particle density ± SD was always much lower in amylase-labeled sections; the labeling density in Golgi apparatus in apo-labeled sections was 42.732 ± 17.239 particles/μm^2 profile area (n = 77) compared to 1.984 ± 4.691 particles/μm^2 profile area (n = 44) in amylase-labeled sections; and the labeling density in large multivesicular endosomes in apoE-labeled sections was 131.913 ± 51.425 particles/μm^2 profile area (n = 89) compared to 0 particles/μm^2 profile area (n = 42) in amylase-labeled sections.

For double-immunolabeling, grids were incubated with both primary antibodies, rabbit anti-apoE and mouse anti-HRP, mixed together in a single step, washed, and the non-specific sites blocked as described above. The grids were then incubated with both secondary antibodies, goat anti-rabbit and goat anti-mouse conjugated to 10 and 5 nm colloidal gold, respectively, in a single step and washed as above. Controls were carried out by omitting either one of the primary antibodies and showed negligible labeling with gold particles corresponding to the omitted antibody (not shown).

The antibodies and gold conjugates were diluted in PBS-BCO. The antibody dilutions were as follows: 1:200 for anti-apoE; 1:40 for anti-CI-MPR; 1:5 for anti-HRP; 1:20 for anti-catalase; 1:10 for anti-albumin; 1:200 for anti-lgp120; 1:5 for goat anti-mouse-5 nm gold; 1:20 for goat anti-rabbit-10 nm gold.

Contrasting and Embedding. To improve the contrast of the frozen sections, a modification of the procedure of Tokuyasu (1978) was used. A 4% uranyl acetate solution was mixed with 0.3 M oxalic acid in a ratio of 1:1. The pH was then adjusted to 7 using 5% ammonium hydroxide. After washing 5 × 2 min with distilled water, the grids were stained for 5 min with uranyl acetate–oxalate solution, rinsed 2 × 1.5 min on drops of distilled water and then transferred onto drops of methyl cellulose containing 0.4% aqueous uranyl acetate for 10 min on ice. After picking up the grids with a 3 mm gold loop, the excess liquid was removed with filter paper and the grids were air dried. Sections were viewed in a Philips 400 T electron microscope, operating at 80 kV.

Analysis of Gold Label. This was carried out essentially as described by Griffiths and Hoppeler (1986). Tissue stubs from respectively, six and four animals were used for the quantitative analysis of apoE and albumin. One to two grids containing sections from one tissue block of each animal were studied. Random fields, with the condition that they be of appropriate thickness (ca. 50 nm) and preservation, were selected at a low magnification (9,000×) at which gold particles were not visible. Section thickness was determined by the method of Small (1968) described in Weibel (1979). Regions of interest were placed in the center of the field. These included the plasmalemmal domains and the cytoplasm in the apical and basolateral domains. The magnification was increased to 15,200 or 22,000× and photographs were taken. Gold particles were counted on prints (at a final magnification of 37,000 or 50,000×).

Gold particles were allocated to the following compartments of liver parenchymal cells: the sinusoidal, lateral, and bile canalicular domains of the plasmalemma, Golgi stacks (including secretory vesicles; <400-nm diam), Golgi-associated vesicles of diameter >400 nm within 100 nm of a Golgi stack, small vesicular profiles between 50–200 nm in diameter (often located in close proximity to the sinusoidal plasmalemma), multivesicular endosome profiles between 200–400 nm and >400 nm in diameter (exhibiting profiles of lipoprotein particles and intraluminal membranes or vesicles), mitochondria, nuclei, peroxisomes, lysosomes, and cytoplasm (including cytosol, endoplasmic reticulum, tubular profiles, and autophagic vacuoles). The micrographs were placed on the measuring tablet of a Zeiss MOP-3 digitizer (Carl Zeiss Inc., Don Mills, Ontario) to determine the profile surface areas of intracellular organelles in μm^2.

Results

Localization of ApoE Immunoreactivity in Liver Cryosections

Using a well-characterized anti-serum to apoE (Wong and Rubenstein, 1977; Wong, 1989) immunogold labeling of cryosections revealed a diffuse distribution along the sinusoidal surface of the plasmalemma with much lower labeling of the lateral plasmalemma or bile canalicular membranes (not shown). Most prominent labeling was observed however in intracellular structures. These included vesicular profiles of various diameters (Fig. 1, *a–g*) as well as the Golgi apparatus and larger Golgi-associated vesicles (Fig. 1, *h–j*). Components of the endocytic apparatus were identified by double labeling for internalized HRP (5 nm gold) and apoE (10 nm gold) (Fig. 2). Endosomes close to the sinusoidal surface (Fig. 2 *a*), multivesicular endosomes near the bile canaliculus (Figs. 2, *b* and *d*), and vesicles of similar morphology in proximity to the Golgi apparatus (Fig. 2 *c*) were double labeled for HRP and apoE. Notably, lysosomes of morphology similar to electron-dense structures positive for the lysosomal marker lgp120 (Fig. 2 *d*, *inset*) were unreactive for apoE (Figs. 2 *d* and 4 *c*). As previously demonstrated by Geuze et al. (1988) and Griffiths et al. (1988), lgp120 is not restricted to secondary lysosomes. Late multivesicular endosomes were also reactive for lgp120 and this was also observed in our studies (Fig. 2 *d*, *inset*, *upper right*).

Analysis of Gold Particle Labeling

The double-labeling studies (Fig. 2 *c*) allowed us to conclude that large profiles of >400 nm in diameter which were apoE labeled and in close proximity to the Golgi apparatus were endosomes (indicated by *asterisks* in Fig. 1, *h–j* as single labeled for apoE, and in Fig. 2 *c* double labeled for apoE and HRP). This enabled therefore the characterization of four size classes of endosomes as illustrated in Fig. 1 with the smaller profiles (50–200 nm in diameter) tending to be near the sinusoidal surface of the hepatocyte. Golgi apparatus was defined as Golgi stacked cisternae with associated small vesicles as illustrated in Fig. 1, *h–j* and 2 *c*.

A summary of the tabulated gold particles is indicated in Fig. 3. The analysis was based on micrographs which were selected on the basis of their morphological preservation but at a magnification where gold particles were not visible (9,000× magnification). Micrographs, taken at a magnification of 15,200 or 22,000× followed by photographic enlargement (37,000 or 50,000×), enabled the determination of the number of gold particles per profile area (μm^2) of each compartment as outlined in the Materials and Methods. Control experiments for non-specific labeling with anti-amylase showed negligible labeling (see Materials and Methods).

Although immunolabeling of cryosections is not considered rigorously quantitative due to problems of antibody penetration (Slot et al., 1989) and antigenic denaturation due to fixation (Lenard and Singer, 1968), gold particle numbers over each profile did follow a relationship proportional to the sectional area of the organellar profile examined at least for endosomes and Golgi apparatus (Fig. 3, *A* and *B*). Such was not the case however, for lysosomes and peroxisomes (Fig. 3 *C*) where no labeling was found. Furthermore, negligible immunolabeling was found over mitochondria, ER, and cytosol (not shown).

In the case of secondary lysosomes the lack of apoE immunoreactivity (cf. Fig. 4 *c*) was unlikely to be due to difficulties in antibody penetration since anti-lgp120 was immunoreactive with secondary lysosomes (Fig. 2 *d*, *inset* and Fig. 4 *d*). Peroxisomes were also unreactive (Figs. 1, *c* and *i*, and 4 *a*) in contrast to the study reported by Hamilton et

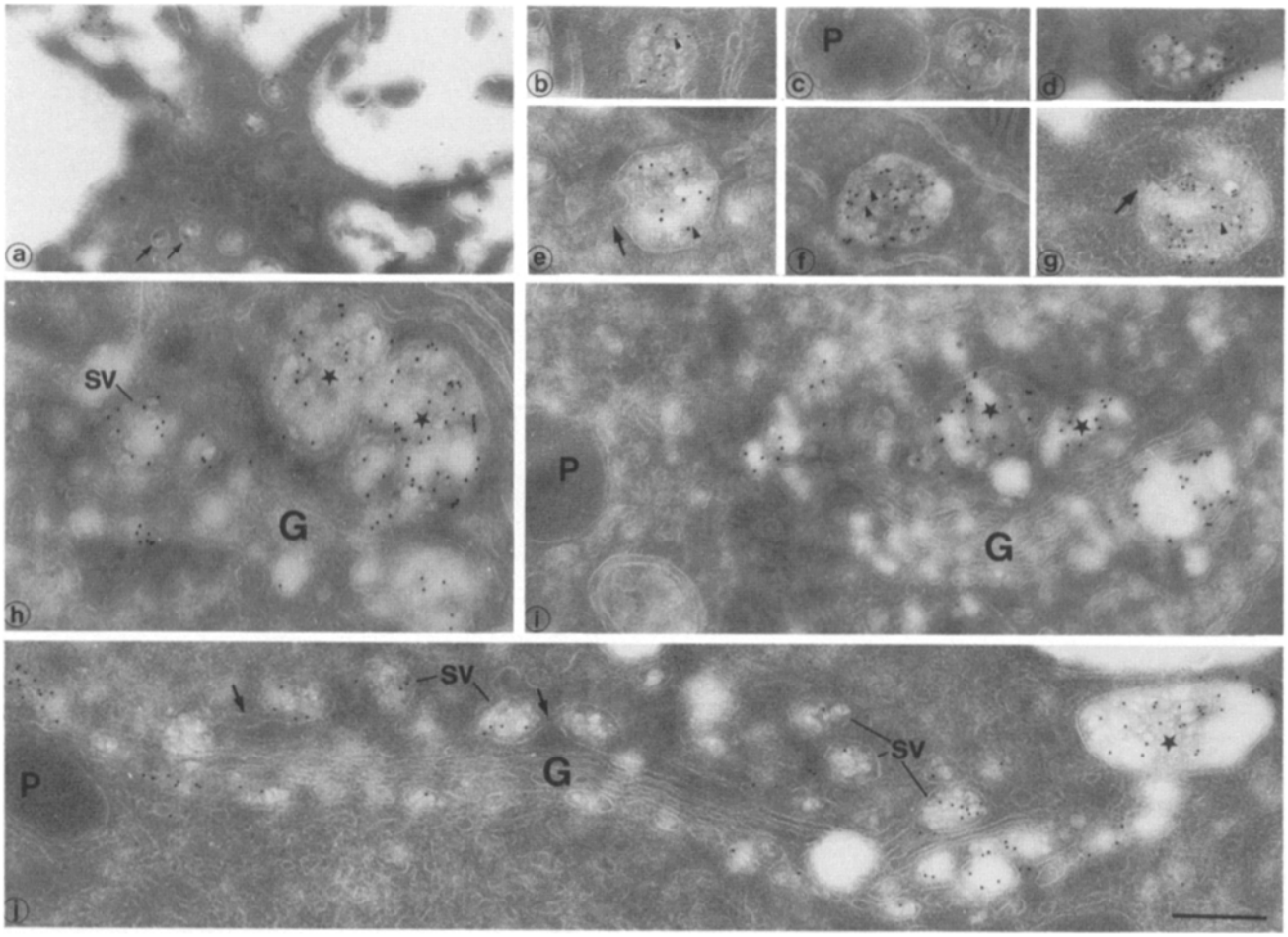

Figure 1. Distribution of apoE in ultrathin cryosections of rat liver. Sections were incubated with a rabbit anti-rat apoE antibody (1:200 dilution) followed by goat anti-rabbit IgG-10 nm gold as described in Materials and Methods. Representative profiles of structures immunoreactive for apoE are shown. (*a*) Two vesicles of 80–100 nm in diameter close to the sinusoidal plasmalemma (*small arrows*). (*b–g*) Examples of multivesicular endosomes 200–400 nm in diameter (*b–d*) and multivesicular endosomes >400 nm in diameter (*e–g*) showing profiles of intraluminal vesicles (*arrowheads*) and tubular appendages (*arrows*). (*h–j*) Stacked Golgi saccules and associated Golgi vesicles of <400 nm in diameter (*sv*). Golgi-associated vesicular profiles (*) of >400 nm in diameter within 100 nm of a Golgi stack (*h–j*) were considered endosomal since they were labeled with internalized HRP (see Fig. 2 *c*). In contrast to multivesicular endosomes however, the Golgi-associated endosomes were usually devoid of intraluminal membrane profiles and intraluminal patches of high electron density. Large arrows (*j*) point to tubular elements emanating from presumptive secretory vesicles. Bar, 0.4 μm.

al. (1990). We feel it unlikely that this represented a problem in antibody penetration since catalase, the peroxisomal marker, was clearly visualized by anti-catalase antibodies while antibody to apoE was unreactive in peroxisomes (cf. Fig. 4, *a* and *b*).

Western Blotting of Purified Organelles of Rat Liver

To evaluate if the lack of immunoreactivity in cytosol, ER, peroxisomes and lysosomes might have been due to selective antigenic inactivation by the fixatives employed in our study, we assessed the distribution of apoE immunoreactivity by Western blotting of purified subcellular fractions. Purified cytosol, ER, endosomes, peroxisomes, mitochondria, an endosome-free Golgi fraction (WNG), a mixed Golgi-endosomal fraction (Gi), a late endosomal fraction uncontaminated with Golgi apparatus (Li), and purified secondary lysosomes (Lys) were prepared following established protocols and where appropriate, an assessment of marker enzyme enrichment (peroxisomes, mitochondria, and Golgi apparatus [WNG], and lysosomes as described in Materials and Methods) was done. Similar to the immunocytochemical findings, negligible immunoreactivity was observed by

Figure 2. Identification of endosomes by internalized horseradish peroxidase. 10 min after the intraportal injection of HRP (*a* and *b*), endocytic structures are found double labeled for endogenous apoE (10 nm gold) and internalized HRP (5 nm gold). The sinusoidal surface (*Sin*) is labeled with 10 nm gold as well as 5 nm gold (*a*). Vesicular profiles near the sinusoidal surface (*end, a*) and other vesicles of varying intraluminal electron density near the bile canaliculus (*bc*), exhibiting a mottled content, are positive for both sized particles. (*c* and *d*) 30 min after the intraportal injection of HRP, large endocytic components closely apposed to the Golgi apparatus (indicated by

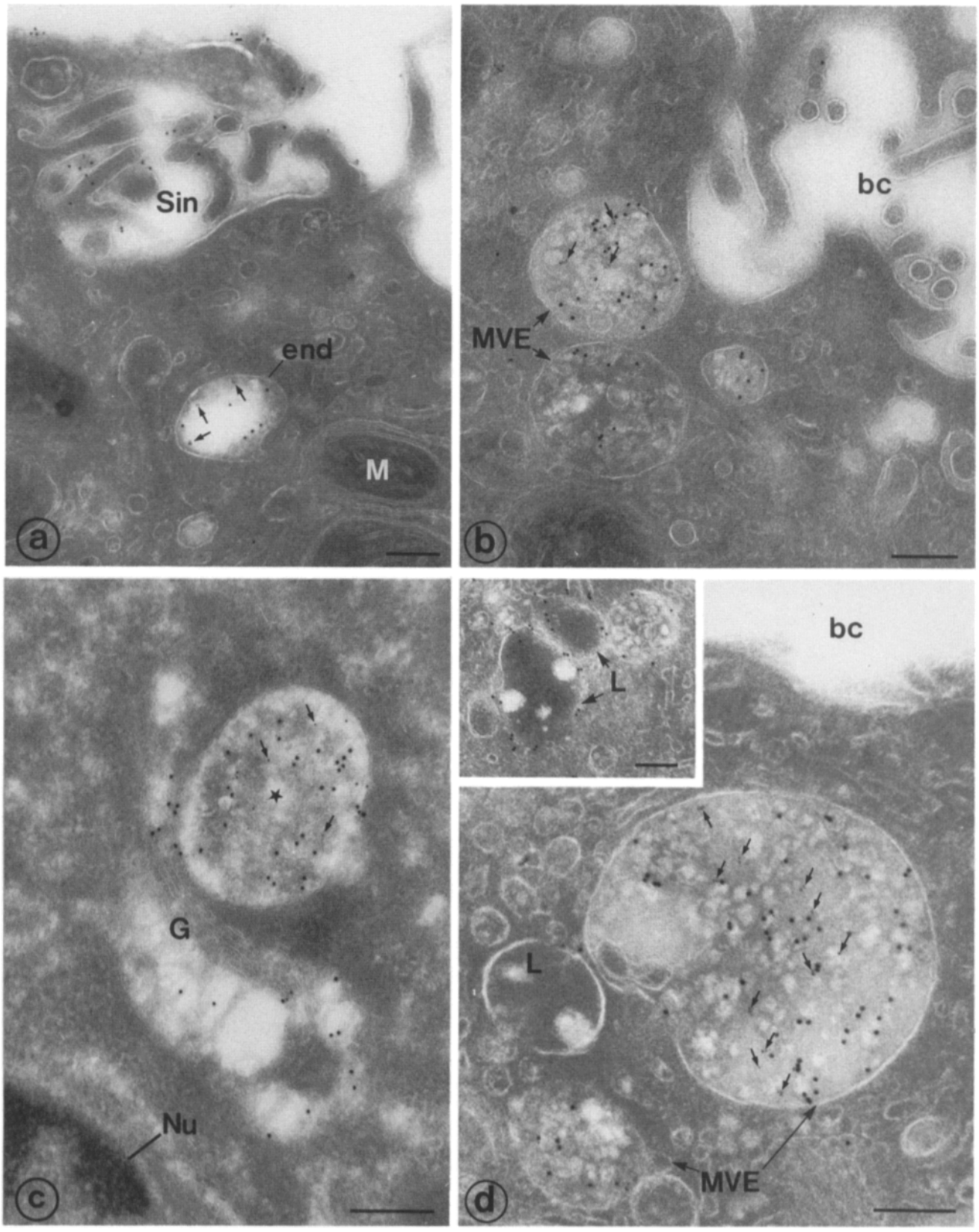

the *asterisk*, *c*) or with a mottled content and intraluminal patches of electron density near the bile canaliculus (multivesicular endosome, *MVE*) (*d*) are double-labeled for apoE (10 nm gold) and internalized HRP (5 nm gold). (*Inset*) Antiserum to the lysosomal marker lgp120 (anti-lgp120) shows labeling with 10 nm gold particles at the periphery of lysosomes (*L*) similar in morphology to that seen in *d*. The lgp-120 reactive lysosomes are adjacent to a late prelysosome (*upper right of inset*) also reactive for lgp-120 at its periphery. *Nu*, nucleus, Bars, 0.2 μm.

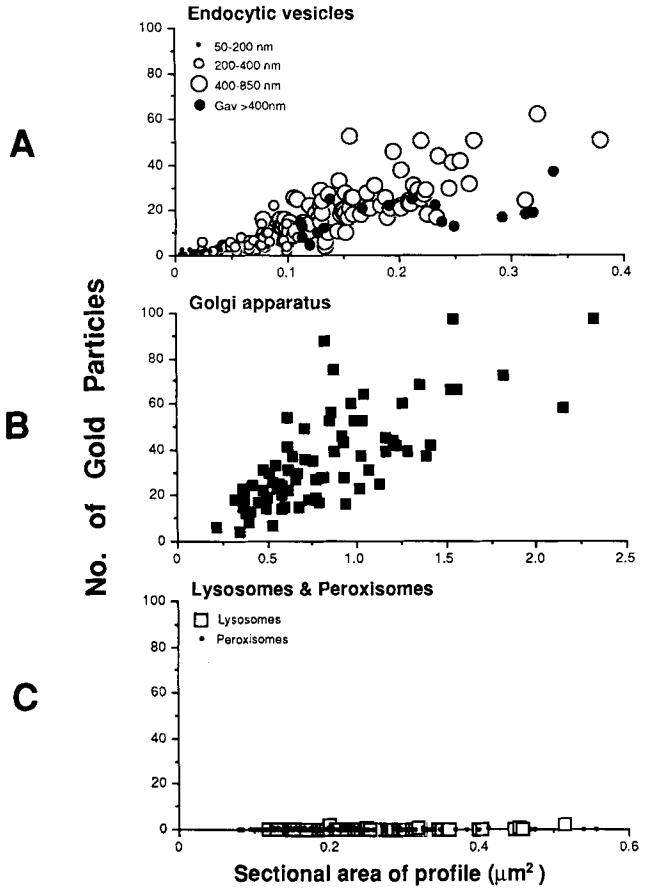

Figure 3. Gold particle labeling of apoE in intracellular organelles. Evaluation of the gold particle number over hepatic endosomes (*A*), Golgi apparatus (*B*), and lysosomes and peroxisomes (*C*) was carried out after immunolabeling with anti-apoE. In *A*, four categories of endocytic structures were evaluated for gold particle number by taking into account their profile area (μm^2). Endosomes were classified as vesicular profiles of 50–200 nm in diameter (●, n = 29), multivesicular endosome profiles of 200–400 nm in diameter (○, n = 35), large multivesicular endosome profiles of 400–850 nm in diameter (○, n = 89) and large vesicular endocytic profiles of >400 nm in diameter in close apposition to the stacked saccules of the Golgi apparatus (●, n = 18). In *B*, 77 profiles of Golgi apparatus (including secretory vesicles, i.e., <400-nm diameter) were scored for gold particle number. Each symbol (■) represents a Golgi apparatus scored. In *C*, 64 lysosomes (□) and 165 peroxisomes (●) were assessed for their gold particle labeling.

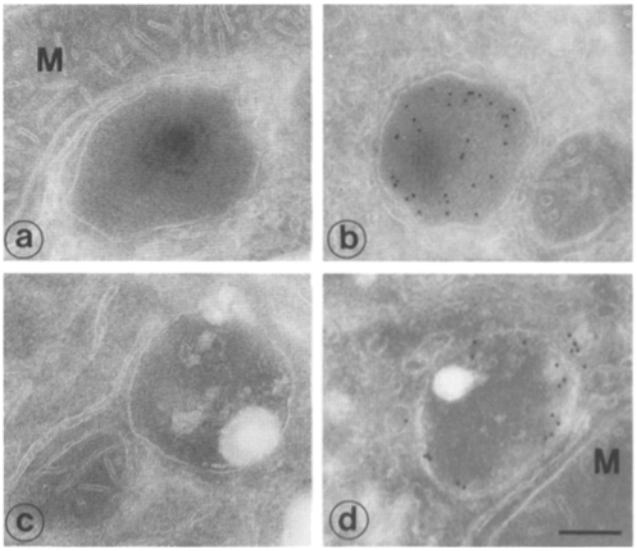

Figure 4. Absence of apoE in peroxisomes and lysosomes. Cryosections were immunolabeled for apoE (*a* and *c*), catalase (*b*), or lgp120 (*d*) with 10 nm gold. Structures having a similar morphology to those harboring the peroxisomal marker, catalase, and the lysosomal marker, lgp120, were negative for apoE. Bar, 0.25 μm.

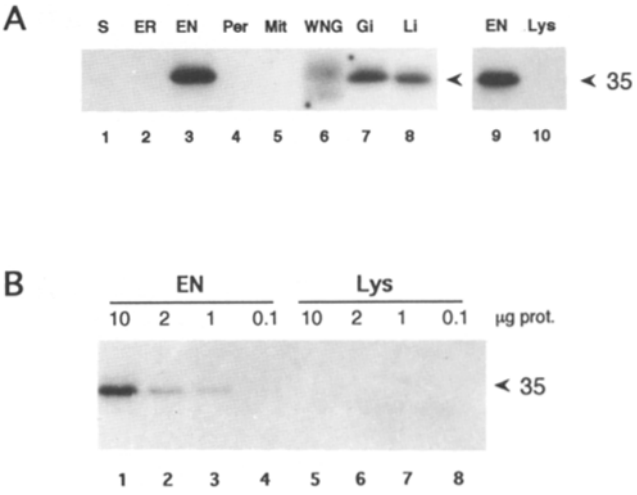

Figure 5. Western blotting of organelles isolated from liver homogenates. (*A*) Cytosolic (*S*), rough endoplasmic reticulum (*ER*), endosomal (*EN*), peroxisomal (*Per*), mitochondrial (*Mit*), Golgi (*WNG*), Golgi endosomal (*Gi*), late endosomal (*Li*), and lysosomal (*Lys*) fractions were processed for immunoblotting with anti-apoE antiserum as described in Materials and Methods. The arrowhead denotes a band of mobility corresponding to ca. 35 kD in molecular mass. There are two immunoreactive bands in the WNG fraction of 29 (*lower*) and 36 kD (*upper*), respectively. These likely represent the unglycosylated precursor and fully glycosylated forms of apoE, respectively. (*B*) Sensitivity of apoE detection by immunoblot. 10 to 0.1 μg of endosomal (*EN*) and lysosomal (*Lys*) fraction protein were processed for immunoblotting with anti-apoE antiserum (1:200). The arrowhead denotes a band of mobility corresponding to ca. 35 kD in molecular mass. ApoE is detectable by the antiserum in as little as 1 μg endosomal fraction protein but is undetectable in 10 μg lysosomal fraction protein.

Western blotting of equal amounts of protein (20 μg) of purified cytosol, ER, peroxisomes, mitochondria, and secondary lysosomes (Fig. 5 *A*). Rather most immunoreactive apoE was found in endosomes and Golgi apparatus.

The WNG Golgi fraction, a highly enriched Golgi fraction largely depleted of endosomes (Rindress et al., 1993) revealed immunoreactive apoE at molecular masses of 29 and 36 kD (Fig. 5 *A*, lane *6*) presumably representing the non-glycosylated and completely O-glycosylated forms of apoE, respectively (Reardon et al., 1986). The Gi fraction consisting of mixed Golgi and endosomal compartments and the Li endosomal fraction (Khan et al., 1986) previously documented to be largely free of Golgi markers and other contaminants, revealed high concentrations of immunoreac-

tive apoE detected at ca. 35 kD by immunoblot analysis (Fig. 5, lanes *7* and *8*). The limit of sensitivity of the immunoblotting protocol was also evaluated. As seen in Fig. 5 *B*, apoE was detected in endosomes using as little as 1 μg of total endosomal protein. By contrast immunoreactivity was undetected in lysosomes at any concentration of protein assessed (Fig. 5 *A*, lane *10*, 20 μg protein; Fig. 5 *B*, lanes *5–8*, 0.1–10 μg protein). The immunoblot of Fig. 5 *B* was assessed at the same dilution of antibody as that used for the immunolabeling studies on cryosections, i.e., within a proportional range of sensitivity of antigenic content in endosomes as shown in Fig. 5 *B*, lanes *1–4*.

Heterogeneous Distribution of ApoE But Not Albumin in Golgi Apparatus

Immunoreactive apoE was not distributed homogeneously throughout the Golgi apparatus (Fig. 1, *h–j*, and Fig. 2 *c*). Rather apoE appeared most concentrated in saccular distensions as well as in small vesicles of 350 nm in diameter at one pole of the Golgi apparatus (Fig. 1, *h–j*, and Fig. 2 *c*). Selection of Golgi apparatus profiles on the basis of their plane of section enabled a comparison of the distribution of apoE with that of the major secretory protein of the hepatocyte, albumin (Figs. 6 and 7). Orientation of the profiles was evaluated morphologically with the *cis–trans* orientation defined by morphological criteria based on the Golgi distribution of the cation-independent mannose 6-phosphate receptor (CI-MPR), a marker of the *trans*-Golgi network (Fig. 6, *g* and *h*). Four compartments of the Golgi apparatus were defined and consisted of Golgi flattened saccules (compartment 1), saccular distensions of ca. 250 nm in diameter (compartment 2), small vesicles of ca. 350 nm in diameter usually at the *trans* pole (compartment 3), and the *trans*-Golgi network (compartment 4). Based on the analysis of Golgi profiles from apoE-labeled sections of livers from six rats and the analysis of 962 gold particles, the majority (55%) were over the saccular distensions but absent in the flattened saccules themselves (Figs. 6, *a* and *b*, and 7 *A*). This contrasted with the distribution of albumin. Assessment of 8747 gold particles of gold-labeled secondary antibody binding to anti-albumin, revealed that immunoreactivity was over all compartments of the Golgi apparatus with no marked heterogeneity observed in its distribution (Figs. 6, *e* and *f*, and 7 *B*) as previously demonstrated by Brands et al. (1983). Hence, apoE appears segregated from albumin in the hepatic Golgi apparatus. In a less extensive study, apoB antigenicity (using anti-rat apoB characterized as in Wong and Pino (1987) and Wong and Torbati (1994)) was restricted to the saccular distensions of the Golgi (Fig. 6, *c* and *d*).

In the above studies, the anti-apoE antiserum was used at 1:200 dilution. However, further experiments were carried out using dilutions of anti-apoE antiserum of 1:50 and 1:25. At these higher concentrations of antiserum, more gold particles were found over all compartments. However, no change in distribution was observed with little labeling found over Golgi apparatus flattened saccules (not shown). Rather, as for Fig. 6 (*a* and *b*) gold particles were restricted to saccular distensions of all Golgi saccules.

Discussion

We have used gold-labeled secondary antibodies to visualize in cryosections of liver parenchyma the intracellular localization of apoE. A complementary approach of preparative subcellular fractionation followed by Western blotting confirmed the conclusions of immunocytochemistry, namely, that at steady state apoE is largely concentrated in components of the endosomal apparatus and Golgi apparatus. Our observations therefore support and extend the previous analytical subcellular fractionation studies of Wong (1989) who concluded that intrahepatic apoE was largely (ca. 65%) endosomal and derived from extracellular sources.

We could delineate four categories of apoE-immunoreactive endosomes with respect to size and location in the cell, all of which contained intraluminal particles which, we propose, represent internalized lipoprotein particles. These particles could be distinguished from intraluminal vesicles which were prominent in very large endosomes (>400 nm) near the bile canaliculus. The juxta-Golgi endosomes (as defined by HRP internalization and within 100 nm of stacked saccules) were also large (>400 nm in diameter) and devoid of intraluminal vesicles or any amorphous content but were enriched in intraluminal lipoprotein-like particles (Figs. 1, *h–j*, 2 *c*). The continuum in gold particle labeling of all four categories of endosomes (Fig. 3 *A*) is suggestive of a relationship whereby endosomes mature by inter-endosomal fusion processes (Stoorvogel et al., 1991; Dunn and Maxfield, 1992). In this regard the close apposition of a subset of endosomes to the Golgi apparatus may be a necessary step in maturation. This would now provide a mechanism for the acquisition of the cation-independent mannose 6-phosphate receptor which is located in the trans Golgi network (Fig. 6, *g* and *h*) and the consequent maturation of endosomes to multivesicular endosomes. The juxta-Golgi category of endosomes in liver parenchyma also explains past work which suggested ^{125}I-labeled insulin (Bergeron et al., 1979, 1985) and ^{125}I-labeled prolactin (Bergeron et al., 1983) uptake in non-lysosomal components closely associated with the Golgi apparatus. More recently, LDL has been concluded to be internalized into vesicles associated with the trans Golgi apparatus (Pathak et al., 1990). Subcellular fractionation studies have previously defined lipoprotein-containing structures concentrating internalized ^{125}I-labeled insulin (Posner et al., 1980; Khan et al., 1982), ^{125}I-labeled prolactin (Josefsberg et al., 1979) and ^{125}I-labeled EGF (Lai et al., 1989) in mixed Golgi–endosome fractions (Kay et al., 1984). Secondary lysosomes, the terminus of the endocytic apparatus showed negligible apoE immunoreactivity whether assessed as lgp120-positive structures with a dense amorphous matrix (Fig. 4 *d*) or as a purified organelle enriched greater than 80-fold in the lysosomal marker acid phosphatase (Fig. 5). This likely indicates the remarkable potency of lysosomes in degrading incoming lipoproteins.

We were unable to detect significant immunoreactivity of apoE in cytosol, ER, mitochondria, peroxisomes, or secondary lysosomes. This was surprising since Hamilton et al. (1990) showed strong gold labeling of cytosol, ER and peroxisomes using a similar immunogold labeling technique. In the case of peroxisomes it is highly unlikely that our lack of detection of apoE was due to a penetration problem with the larger gold-labeled secondary antibody as opposed to the smaller protein A–gold probe used by Hamilton et al. (1990) since we were able to demonstrate immunogold labeling of peroxisomes with anti-catalase (Fig. 4 *b*). Our

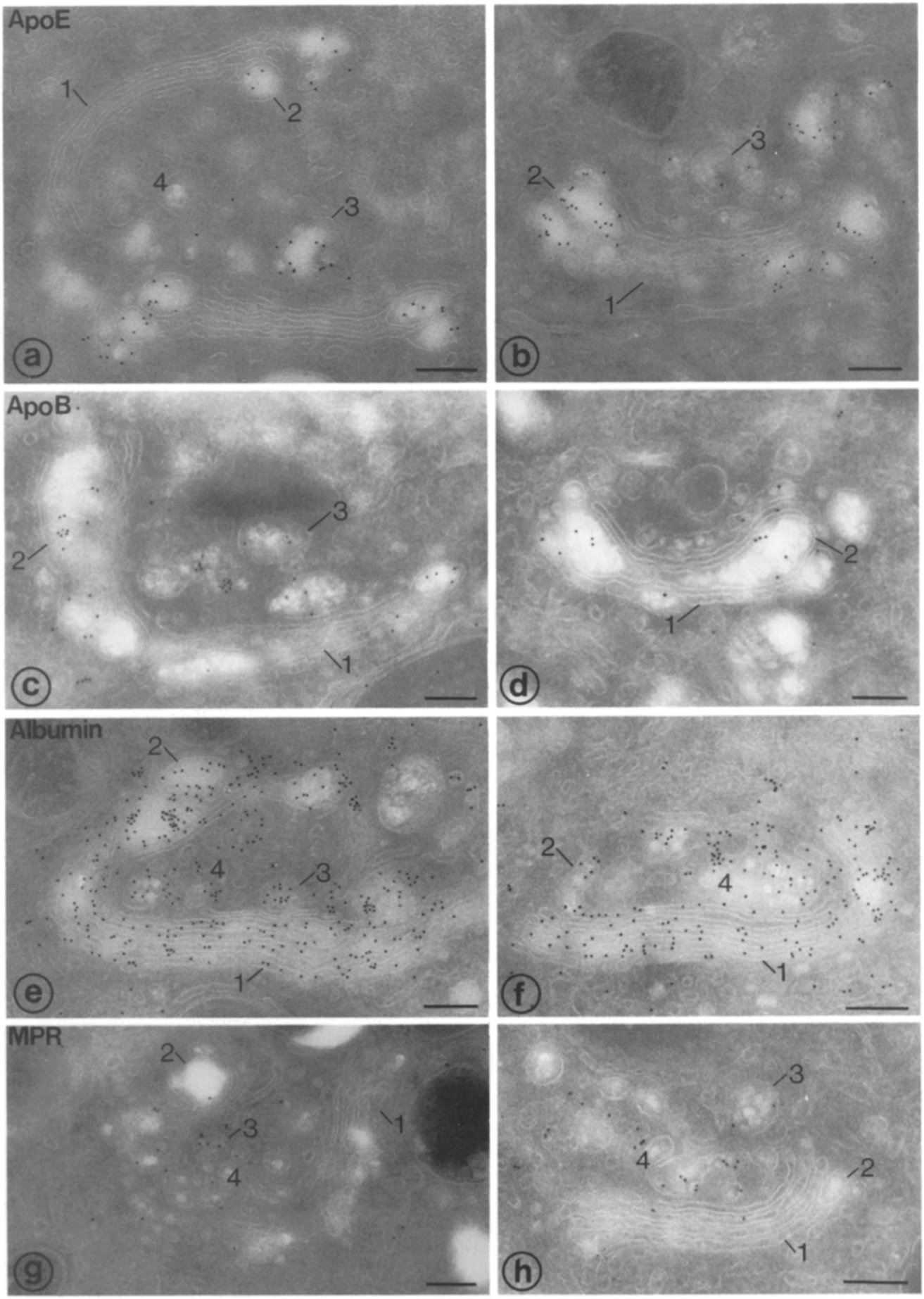
ApoE
1
2
4
3
a
3
2
1
b
ApoB
3
2
1
c
2
1
d
Albumin
2
4
3
1
e
2
4
1
f
MPR
2
3
1
4
g
3
4
2
1
h

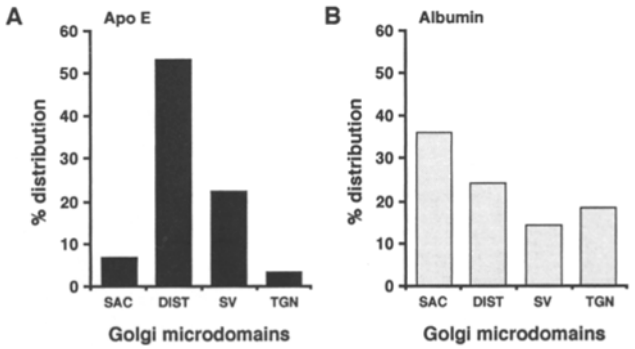

Figure 7. Percent distribution of gold particles in Golgi microdomains. Cross-sectional profiles of Golgi apparatus were evaluated for the distribution of apoE (*A*) or albumin (*B*) immunoreactivity in microdomains as indicated in the legend to Fig. 6. A total of 962 and 8,747 particles were counted over 26 and 46 profiles of Golgi apparatus that were labeled for apoE or albumin, respectively. Gold particles in the vicinity of the Golgi profiles over components which could not be clearly ascribed to any of the above microdomains comprised 14.9 and 7.6% of the total number of particles counted over apoE- and albumin-labeled Golgi apparatus, respectively. Gold particles denoting apoE content are concentrated in the peripheral distentions of Golgi saccules, while albumin is diffusely distributed throughout the Golgi apparatus. The distributions were compared by statistical analysis and found to be significantly different (chi square = 84.07, $P < 0.001$).

results were also confirmed by Western blot analysis of highly purified peroxisomes (>90% as documented by Bodmer and Rachubinski, 1991, and characterized by Authier et al., 1994) which showed negligible apoE immunoreactivity. Since purified cytosol, ER, and mitochondria also showed negligible apoE immunoreactivity our studies do not support the hypothesis of Hamilton et al. (1990) that apoE could serve as an intracellular sterol carrier responsible for shuttling cholesterol among intracellular organelles including peroxisomes. Indeed, for peroxisomes, an unrelated sterol carrier protein has been recently identified which possesses both type I and type II peroxisomal targetting motifs (Ossendorp and Wirtz, 1993) neither of which are found in any isoform of apoE so far described (Zannis and Breslow, 1981; Zannis et al., 1981, 1984; Wallis et al., 1983; Das et al., 1985; Paik et al., 1985; Reardon et al., 1986; Zannis, 1986).

Within the Golgi apparatus, apoE was clearly distributed differently to that of albumin. Whereas the latter was uniformly distributed throughout the stacked saccules and bulbous distensions, apoE was restricted to the peripheral distensions (ca. 250 nm in diameter). Similar observations were also found for apoB, the other major protein constituent of VLDL (Fig. 6, *c* and *d*). Intra-Golgi segregation of apoE was observed in distensions of all saccules of the hepatic Golgi apparatus. These observations are reminiscent of the intra-Golgi segregation of collagen in connective tissue fibroblasts, osteoblasts, and odontoblasts as observed morphologically as well as by EM immunocytochemistry (reviewed by Leblond, 1989). The intra-Golgi segregation of apoE into Golgi saccular distensions that we have observed may be relevant to the sorting of newly synthesized heparan sulfate proteoglycans into distinct post-TGN vesicular carriers to those containing newly synthesized albumin in rat hepatocytes (Nickel et al., 1994). Our observations are also relevant to current theories on the mechanism of intra-Golgi transport. No apoE- (or albumin-) reactive vesicles of the size expected to be intra-Golgi vesicular carriers (70 nm; Rothman and Orci, 1992) were observed in our studies. While we cannot exclude the possibility that such vesicles are refractory to the penetration of gold labeled antibodies we find this unlikely since no such difficulty was observed in Golgi flattened saccules where only a 25 nm distance defines the luminal space of cross-sectioned Golgi cisternae (Fig. 6). Recent work of Clermont et al. (1993) has indicated that small (80 nm) vesicles about the Golgi apparatus of lactating mammary gland were devoid of secretory casein submicelles while this secretory content was clearly observed in distended portions of Golgi saccules. Past studies of Leblond and colleagues (reviewed in Leblond, 1989) have demonstrated the packaging of collagen in saccular distensions of Golgi apparatus of collagen-producing connective tissue fibroblasts as well as osteoblasts and odontoblasts but these investigators were also unable to detect collagen in small Golgi vesicles. As indicated by Mellman and Simons (1992) the lack of detection of secretory material in vesicular structures adjacent to Golgi cisternae raises questions about the postulated role of such vesicles in the forward reaction of intra-Golgi transport.

The authors would like to thank Drs. A. G. Bodnar and R. A. Rachubinski for preparing the peroxisomal and mitochondrial fractions used in this study. As well, we thank Dr. I. Mellman for the antiserum to lgp120, Dr. P. Nissley for the anti-MPR antibody, and Dr. M. Bendayan for the anti-α amylase antibody. We are grateful to Dr. F. Authier and Ali Fazel for their help in preparing the lysosomal fractions and in the immunoblotting study. We thank Ms. J. Mui for cryosectioning and photography. Also, we are particularly indebted to Drs. Y. Clermont and C. E. Smith for helpful discussions and for critically reading the manuscript.

Supported by grants from the Medical Research Council of Canada (J. J. M. Bergeron and B. I. Posner) and National Institutes of Health grant HL 25596 (L. Wong). J. P. Ahluwalia was supported by a studentship from Fonds de la Recherche en Santé du Québec during the course of this work.

Received for publication 1 July 1994 and in revised form 27 September 1994.

References

Authier, F., R. A. Rachubinski, B. I. Posner, and J. J. M. Bergeron. 1994. Endosomal proteolysis of insulin by an acidic thiol-metalloprotease unrelated to insulin degrading enzyme. *J. Biol. Chem.* 269:3010–3016.

Bendayan, M. 1984. Concentration of amylase along its secretory pathway in the pancreatic acinar cell as revealed by high resolution immunocytochemistry. *Histochem. J.* 16:85–108.

Bergeron, J. J. M., R. Sikstrom, A. R. Hand, and B. I. Posner. 1979. Binding and uptake of ^{125}I-insulin into rat liver hepatocytes and endothelium. *J. Cell*

Figure 6. Heterogeneous distribution of apoE but not albumin in Golgi apparatus. Cryosections were immunolabeled for apoE (*a* and *b*), apoB (*c* and *d*), rat albumin (*e* and *f*) or CI-MPR (*g* and *h*). Microdomains of the Golgi apparatus in which gold particles were evaluated are indicated by the numbers 1–4. The regions are defined as: (*1*) flattened saccules; (*2*) saccular distentions; (*3*) secretory vesicles; and (*4*) TGN, i.e., the *trans*-Golgi network (as defined by CI-MPR-labeling, *g* and *h*). Albumin is seen to be diffusely distributed throughout the Golgi while apoE and apoB are concentrated in the saccular distentions. Bars, 0.25 μm.

Biol. 80:427–443.
Bergeron, J. J. M., L. Resch, R. Rachubinski, B. A. Patel, and B. I. Posner. 1983. Effect of colchicine on internalization of prolactin in female rat liver: an in vivo radioautographic study. *J. Cell Biol.* 96:875–886.
Bergeron, J. J. M., J. Cruz, M. N. Khan, and B. I. Posner. 1985. Uptake of insulin and other ligands into receptor-rich endocytic components of target cells: the endosomal apparatus. *Annu. Rev. Physiol.* 47:383–403.
Bodnar, A. G., and R. A. Rachubinski. 1991. Characterization of the integral membrane polypeptides of rat liver peroxisomes isolated from untreated and clofibrate-treated rats. *Biochem. Cell Biol.* 69:499–508.
Bradford, M. M. 1976. A rapid and sensitive method for the quantitation of microgram quantities of protein utilizing the principle of protein-dye binding. *Anal. Biochem.* 72:248–254.
Brands, R., J. W. Slot, and H. J. Geuze. 1983. Albumin localization in rat liver parenchymal cells. *Eur. J. Cell Biol.* 32:99–107.
Claude, A. 1970. Growth and differentiation of cytoplasmic membranes in the course of lipoprotein granule synthesis in the hepatic cell. I. Elaboration of elements of the Golgi complex. *J. Cell Biol.* 47:745–766.
Clermont, Y., L. Xia, A. Rambourg, J. D. Turner, and L. Hermo. 1993. Transport of casein submicelles and formation of secretion granules in the Golgi apparatus of epithelial cells of the lactating mammary gland of rat. *Anat. Rec.* 235:363–373.
Das, H. K., J. McPherson, G. A. P. Bruns, S. K. Karathanasis, and J. L. Breslow. 1985. Isolation, characterization, and mapping to chromosome 19 of the human apolipoprotein E gene. *J. Biol. Chem.* 260:6240–6247.
Dunn, K. W., and F. R. Maxfield. 1992. Delivery of ligands from sorting endosomes to late endosomes occurs by maturation of sorting endosomes. *J. Cell Biol.* 117:301–310.
Ehrenreich, J. H., J. J. M. Bergeron, P. Siekevitz, and G. E. Palade. 1973. Golgi fractions prepared from rat liver homogenates. I. Isolation procedure and morphological characterization. *J. Cell Biol.* 59:45–72.
Geuze, H. J., J. W. Slot, K. T. Tokuyasu, W. E. M. Goedemans, and J. M. Griffith. 1979. Immunocytochemical localization of amylase and chymotrypsin in the exocrine pancreatic cell with special attention to the Golgi complex. *J. Cell Biol.* 82:697–707.
Geuze, H. J., J. W. Slot, G. J. A. M. Strous, J. Peppard, K. M. Figura, A. Hasilik, and A. L. Schwartz. 1984. Intracellular receptor sorting during endocytosis: Comparative immunoelectron microscopy of multiple receptors in rat liver. *Cell.* 37:195–204.
Geuze, H. J., W. Stoorvogel, G. J. Strous, J. W. Slot, J. E. Bleekemolen, and I. Mellman. 1988. Sorting of mannose 6-phosphate receptors and lysosomal membrane proteins in endocytic vesicles. *J. Cell Biol.* 107:2491–2501.
Griffiths, G., and H. Hoppeler. 1986. Quantitation in immunocytochemistry: Correlation of immunogold labeling to absolute number of membrane antigens. *J. Histochem. Cytochem.* 34:1389–1398.
Griffiths, G., R. Brands, B. Burke, D. Louvard, and G. Warren. 1982. Viral membrane proteins acquire galactose in *trans*-Golgi cisternae during intracellular transport. *J. Cell Biol.* 95:781–792.
Griffiths, G., K. Simons, G. Warren, and K. T. Tokuyasu. 1983. Immunoelectron microscopy using thin, frozen sections: application to studies of intracellular transport of Semliki Forest virus spike glycoproteins. *Methods Enzymol.* 96:466–483.
Griffiths, G., A. McDowall, R. Back, and J. Dubochet. 1984. On the preparation of cryosections for immunocytochemistry. *J. Ultrastruct. Res.* 89: 65–78.
Griffiths, G., B. Hoflack, K. Simons, I. Mellman, and S. Kornfeld. 1988. The mannose 6-phosphate receptor and the biogenesis of lysosomes. *Cell.* 52:329–341.
Haimes, H. B., R. J. Stochert, A. G. Morell, and A. B. Novikoff. 1981. Carbohydrate specified endocytosis: localization of ligand in the lysosomal compartment. *Proc. Natl. Acad. Sci. USA.* 78:6936–6939.
Hamilton, R. L., J. S. Wong, L. S. S. Guo, S. Krisans, and R. J. Havel. 1990. Apolipoprotein E localization in rat hepatocytes by immunogold labeling of cryothin sections. *J. Lipid Res.* 31:1589–1603.
Josefsberg, Z., B. I. Posner, B. Patel, and J. J. M. Bergeron. 1979. The uptake of prolactin into female rat liver: Concentration of intact hormone in the Golgi apparatus. *J. Biol. Chem.* 254:209–214.
Kay, D. G., M. N. Khan, B. I. Posner, and J. J. M. Bergeron. 1984. ^{125}I-insulin in hepatic Golgi fractions: application of the diaminobenzidine (DAB)-shift protocol. *Biochem. Biophys. Res. Commun.* 123:1144–1148.
Khan, M. N., B. I. Posner, R. J. Khan, and J. J. M. Bergeron. 1982. Internalization of insulin into rat liver Golgi elements: evidence for vesicle heterogeneity and the path of intracellular processing. *J. Biol. Chem.* 257: 5969–5976.
Khan, M. N., S. Savoie, J. J. M. Bergeron, and B. I. Posner. 1986. Characterization of rat liver endosomal fractions: in vivo activation of insulin stimulable receptor kinase in these structures. *J. Biol. Chem.* 261:8462–8472.
Lai, W. H., P. H. Cameron, J. J. Doherty, II, B. I. Posner, and J. J. M. Bergeron. 1989. Ligand-mediated autophosphorylation activity of the epidermal growth factor receptor during internalization. *J. Cell Biol.* 109:2751–2760.
Leblond, C. P. 1989. Synthesis and secretion of collagen by cells of connective tissue, bone, and dentin. *Anat. Rec.* 224:123–138.
Lenard, J., and S. J Singer. 1968. Alterations of the conformation of proteins in red blood cell membranes and in solutions by fixatives used in electron microscopy. *J. Cell Biol.* 37:117–121.
Mellman, I., and K. Simons. 1992. The Golgi complex: in vitro veritas? *Cell.* 68:829–840.
Nickel, W., L. A. Huber, R. A. Kahn, N. Kipper, A. Barthel, D. Fasshauer, and H.-D. Soling. 1994. ADP ribosylation factor and a 14-kD polypeptide are associated with heparan sulfate-carrying post-trans-Golgi network secretory vesicles in rat hepatocytes. *J. Cell Biol.* 125:721–732.
Novikoff, P. M., and A. Yam. 1978. Sites of lipoprotein particles in normal rat hepatocytes. *J. Cell Biol.* 76:1–11.
Ossendorp, B. C., and K. W. A. Wirtz. 1993. The non-specific lipid-transfer protein (sterol carrier protein 2) and its relationship to peroxisomes. *Biochimie.* 75:191–200.
Ou, W.-J., D. Y. Thomas, A. W. Bell, and J. J. M. Bergeron. 1992. Casein kinase II phosphorylation of signal sequence receptor alpha and the associated membrane chaperone calnexin. *J. Biol. Chem.* 267:23789–23796.
Paik, Y. K., D. J. Chang, C. A. Reardon, G. E. Davies, R. W. Mahley, and J. M. Taylor. 1985. Nucleotide sequence and structure of the human apolipoprotein E gene. *J. Biol. Chem.* 260:6240–6246.
Palade, G. 1975. Intracellular aspects of the process of protein secretion. *Science (Wash. DC).* 189:347–358.
Pathak, R. K., M. Yokode, R. E. Hammer, S. L. Hofmann, M. S. Brown, J. L. Goldstein, and R. G. W. Anderson. 1990. Tissue-specific sorting of the human LDL receptor in polarized epithelia of transgenic mice. *J. Cell Biol.* 111:347–359.
Posner, B. I., B. Patel, A. K. Verma, and J. J. M. Bergeron. 1980. Uptake of insulin by plasmalemma and Golgi subfractions of rat liver. *J. Biol. Chem.* 255:735–741.
Posner, B. I., B. A. Patel, and J. J. M. Bergeron. 1982. Effect of chloroquine on the internalization of ^{125}I-insulin into subcellular fractions of rat liver: evidence for an effect of chloroquine on Golgi elements. *J. Biol. Chem.* 257:5789–5799.
Reardon, C. A., D. M. Driscoll, R. A. Davis, R. A. Borchardt, and G. S. Getz. 1986. The charge polymorphism of rat apoprotein E. *J. Biol. Chem.* 261:4638–4645.
Rindress, D., X. Lei, J. P. Ahluwalia, P. H. Cameron, A. Fazel, B. I. Posner, and J. J. M. Bergeron. 1993. Organelle-specific phosphorylation: identification of unique membrane phosphoproteins of the endoplasmic reticulum and endosomal apparatus. *J. Biol. Chem.* 268:5139–5147.
Rothman, J. E., and L. Orci. 1992. Molecular dissection of the secretory pathway. *Nature (Lond.).* 355:409–415.
Rothman, S. S. 1975. Protein transport by the pancreas. *Science (Wash. DC).* 190:747–753.
Slot, J. W., G. Posthuma, L.-Y. Chang, J. D. Crapo, and H. J. Geuze. 1989. Quantitative aspects of immunogold labeling in embedded and nonembedded sections. *Am. J. Anat.* 185:271–281.
Small, J. V. 1968. Measurement of section thickness. *In* Proceedings of the 4th European Congress on Electon Microscopy. Vol. 1. D. S. Bocciarelli, editor. Tipographia Poliglotta Vaticana, Rome, Italy. 609 pp.
Stoorvogel, W., G. J. Strous, H. J. Geuze, V. Oorschot, and A. L. Schwartz. 1991. Late endosomes derive from early endosomes by maturation. *Cell.* 65:417–427.
Tokuyasu, K. T. 1978. A study of positive staining for ultrathin frozen sections. *J. Ultrastruc. Res.* 63:287–307.
Tokuyasu, K. T. 1980. Immunochemistry on ultrathin frozen sections. *Histochem. J.* 12:381–403.
Towbin, H., T. Staehelin, and J. Gordon. 1979. Electrophoretic transfer of proteins from polyacrylamide to nitrocellulose sheets: procedure and some applications. *Proc. Natl. Acad. Sci. USA.* 76:4350–4354.
Wada, I., D. Rindress, P. H. Cameron, W.-J. Ou, J.-J. Doherty, II, D. Louvard, A. W. Bell, D. Dignard, D. Y. Thomas, and J. J. M. Bergeron. 1991. SSR alpha and associated calnexin are major calcium binding proteins of the endoplasmic reticulum membrane. *J. Biol. Chem.* 266:19599–19610.
Wall, D. A., G. Wilson, and A. L. Hubbard. 1980. The galactose-specific recognition system of mammalian liver: the route of ligand internalization in rat hepatocytes. *Cell.* 21:79–93.
Wallis, S. C., S. Rogne, L. Gill, A. Markham, M. Edge, D. Woods, R. Williamson, and S. Humphries. 1983. The isolation of cDNA clones for human apolipoprotein E and the detection of apoE RNA in hepatic and extra-hepatic tissues. *EMBO (Eur. Mol. Biol. Organ.) J.* 2:2369–2373.
Walter, P., and G. Blobel. 1983. Preparation of microsomal membranes for cotranslational protein translocation. *Methods Enzymol.* 96:84–93.
Wattiaux, R., S. Wattiaux-de Coninck, M.-F. Ronveaux-Dupal, and F. Dubois. 1978. Isolation of rat liver lysosomes by isopynic centrifugation in a metrizamide gradient. *J. Cell Biol.* 78:349–368.
Weibel, E. W. 1979. Stereological Methods: Practical Methods for Biological Morphometry. Vol. 1. Academic Press, New York. 148–149.
Wong, L. 1989. Contribution of endosomes to intrahepatic distribution of apolipoprotein B and apolipoprotein E. *J. Cell. Physiol.* 141:441–452.
Wong, L., and D. Rubinstein. 1977. The levels of apolipoprotein-E in hypercholesterolemic rat serum. *Can. J. Biochem.* 56:161–165.
Wong, L., and R. M. Pino. 1987. Biogenesis of very-low-density lipoproteins in rat liver. Intracellular distribution of apolipoprotein B. *Eur. J. Biochem.* 164:357–367.
Wong, L., and A. Torbati. 1994. Differentiation of intrahepatic membrane-

bound and secretory apolipoprotein B by monoclonal antibodies: membrane-bound apolipoprotein B is more glycosylated. *Biochemistry.* 33:1923–1929.
Zannis, V. I. 1986. Genetic polymorphism in human apolipoprotein E. *Methods Enzymol.* 128:823–851.
Zannis, V. I., and J. L. Breslow. 1981. Human very low density lipoprotein apolipoprotein E isoprotein polymorphism is explained by genetic variation and posttranslational modification. *Biochemistry.* 20:1033–1041.
Zannis, V. I., P. W. Just, and J. L. Breslow. 1981. Human apolipoprotein E isoprotein subclasses are genetically determined. *Am. J. Hum. Genet.* 33:11–24.
Zannis, V. I., J. McPherson, G. Goldberger, S. K. Karathanasis, and J. L. Breslow. 1984. Synthesis, intracellular processing, and signal peptide of human apolipoprotein E. *J. Biol. Chem.* 259:5495–5499.
Zannis, V. I., D. Kardasis, and E. Zanni. 1993. Genetic mutations affecting human lipoproteins, their receptors and their enzymes. *In* Advances in Human Genetics. H. Harris and K. Hirschbom, editors. Vol. 21. Plenum Press, New York. 145–319.